Towards All-Carbon molecular electronic devices

Final Master Project

2015-2016

Aitor García Serrano

Physical Chemistry Department

Research group: PLATÓN (E-54)

Director: Pilar Cea Mingueza

INDEX

Abstract

The development of electronic devices smaller in size, with higher efficiency and low cost has become one a main objective in the micro and nanoelectronics industry in the last years. Due to the scarceness of raw materials used in electronic devices as well as their high cost the search for all-organic electronic devices is a priority. Good examples in the organic electronics industry include organic light emitting diodes and plastic photovoltaic cells. In this final master project, we extend this idea to the field of molecular electronics. Thus, an *in situ* synthesis of diazonium salts from their corresponding amines has been carried out. Thereafter, we have prepared films of controlled thickness by means of an *electrografting* process onto highly oriented pyrolytic graphite (HOPG) electrodes. The terminal trimethylsilane (TMS) group in the organic material used has shown its significance as protector group, preventing multilayer formation. In addition, electrochemistry, atomic force microscopy (AFM), X-ray photoelectron spectroscopy (XPS) and RAMAN characterization has provided information about the thickness of the film, the blocking degree of the substrate (thanks to the different information that can be obtained from the electrochemical response of potassium hexacyanoferrate (III) and dopamine redox probes), the resulting morphology (staring at the roughness or the thickness of the film) and the final chemical composition of the layer. Finally, a carbon top-contact electrode has been deposited onto the organic monolayer and the electrical circuit closed. The electric properties of these nascent carbon electrode/monolayer/carbon electrode devices were measured.

1. Introduction to Molecular Electronics

Nowadays our society demands more efficient and faster electronic devices. Thus, there has been a miniaturization process of the hardware components for the last sixty years, since the transistor computers began to be developed. Our present electronic technology is based in silicon, but due to both the technological and economical limitations,[1] it is necessary to develop new technologies that permit the construction of devices below 10 nm in size. One of the technologies under study is Molecular Electronics. Molecular Electronics is based on the concept of using organic molecules as wires, rectifiers, diodes, plugs, etc. Thus, in 1974, Arieh Aviram and Mark Ratner,[2] workers from the investigation center Thomas J. Watson, New York, suggested that a molecule could work as a rectifier. Since this year, the scientific community has studied the electronic transport in organic molecules and the quantic effects associated, proving that a single molecule or a monolayer can conduct and commute the electric current.[3]

Up to now, most of the scientific literature published in the field of Molecular Electronics is based in the use of metallic electrodes (principally gold) where organic molecules with terminal groups such as thiols can be chemisorbed onto the substrate. But some scientists[4] have recently begun to require a cheaper technology, avoiding the use of metallic electrodes, and move towards the use of organic electrodes (Figure 1), that can be made flexible, transparent and, hopefully, could improve the charge transfer in the electrode-molecule interface. Such an evolution is evident in the field of Organic Electronics, which has moved in the last years towards the development of optoelectronic devices or photovoltaic cells using low cost organic substrates. Another important reason to avoid the use of metals in Molecular Electronics is the quenching process induced by metals in optoelectronic devices.

There are different methods to deposit a monolayer onto a surface. The most used in the field of Molecular Electronics include the Langmuir-Blodgett (LB) and the Self-Assembly (SA) techniques as well as *electrografting* methods.[5]

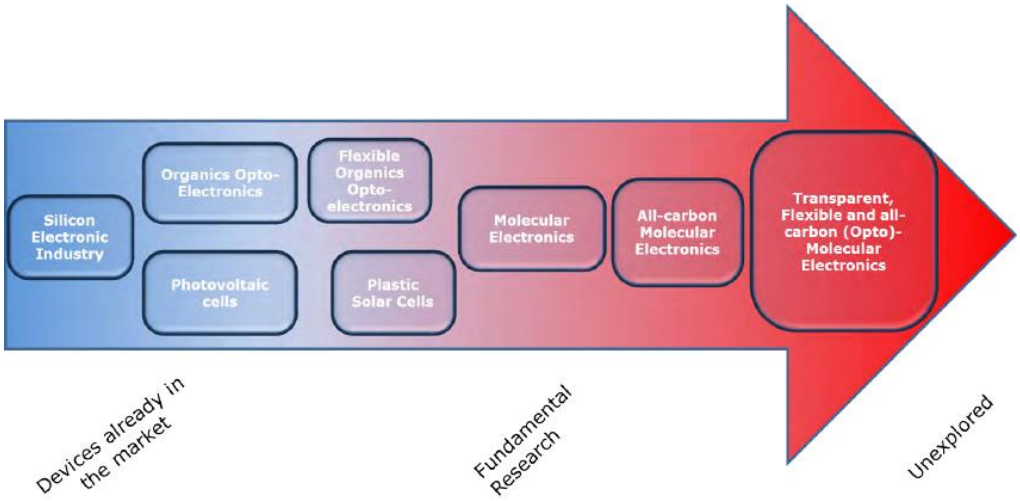

Figure 1. Research activity evolution in electronics, optoelectronics and molecular optoelectronics. Taken from "*Nanofabrication techniques of highly organized monolayers sandwitched between two electrodes for molecular electronics*".[6]

The *electrografting* process allows the formation of covalent bonds C-C between the substrate and the molecule when a current is applied to the electrode and then, thanks to an electrochemistry process, the reaction takes place. It is necessary to emphasize that the important achievement here is the formation of a covalent bond between the substrate and the molecule, which is expected to result in an improvement of the electron transport in the device. One of the most common terminal groups used in the *electrografting* process has been the diazonium salt (Figure 2).[7]

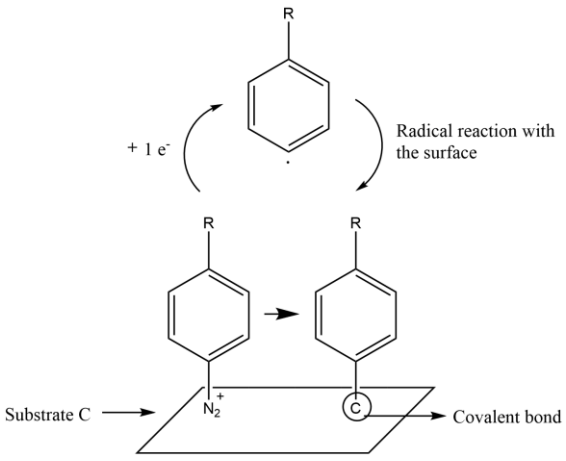

Figure 2. Reaction mechanism of a diazonium salt and formation of an organic layer onto a conducting substrate.

This process has hardly been applied in Molecular Electronics applications due to different problems associated to the mechanism and the process per se. One of the problems is the three-dimensional (3D) growing of the coating and the formation of multilayers of different thickness. Another limitation is the incomplete coating of the surface, because is not easy to obtain a film without pores or defects. These are the reasons why the process has not been successfully used to create a good monolayer onto a substrate, but in the last years different approximations were applied, which include the use of inhibitors[8] or the modification of positions 3 and 5 of an aromatic terminal ring[9] to avoid the 3D growing. Another approximation used before in the PLATON research group from the University of Zaragoza,[10] was to modify the position 4 of an aromatic terminal ring by introducing a bulky group: a trimethylsilane (TMS) group. The TMS group avoids the multilayer formation since it makes difficult the approximation of other molecules due to the steric hindrance of this bulky group. Finally, the molecule that is going to be applied for Molecular Electronics must be conductive. The PLATON research group has a large experience with different molecules which contain the oligo phenylene ethynylene (OPE) moiety,[11] commonly used as a benchmark in Molecular Electronics due to its high conductivity.

Figure 3 shows the molecular structure of the compound used in this work, henceforward abbreviated as TMS-OPE-NH_2

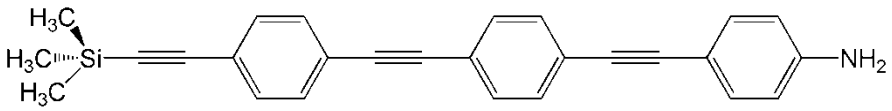

Figure 3. Chemical structure of 4-(4-(4-(trimethylsilylethynyl)phenylethynyl)phenylethynyl) aniline, abbreviated as TMS-OPE-NH_2.

The *electrografting* process of TMS-OPE-NH_2 has been studied in previous works[10] by the PLATON research group and has been deposited onto different substrates including glassy carbon, Highly Ordered Pyrolytic Graphite (HOPG) or poly(3,4-ethylenedioxythiophene) polystyrene sulfonate (PEDOT:PSS). The next step in the optimization process to form a homogeneous monolayer where all molecules are chemically bond to the carbon-based electrode is the removal of the TMS group. This step

is required to ensure the formation of a C-C bond with the substrate (avoiding the presence of physisorbed material) and also to limit the formation of multilayers[12] (Figure 4).

2. Objectives

This work has an educational part as corresponds to a final master project. Thus, for the progress of this work, the scientific method has been applied by the master student, using principles and concepts not only from Physical Chemistry, but also from Organic Chemistry and Physics. As an educational subject, I consider that I have achieved an important autonomy degree with a critic mind which has helped me to solve scientific problems encountered trough the development of this project. Finally, another purpose of this final mater project is to be able to communicate the knowledge achieved through this report, as well as in the oral presentation of this final master project.

The scientific objectives of this final master project are focused in the fabrication of all-carbon molecular electronic devices. An *electrografting* process from a diazonium salt, which was *in situ* synthetized, was used to deposit a monolayer of a conductive organic compound onto a HOPG substrate. Subsequently, these films were characterized by electrochemical and spectroscopic techniques, as well as by atomic force microscopy (AFM). Once the monolayer was formed a top-contact electrode was deposited by means of focused electron beam induced deposition (C-FEBID). Finally, *I-V* curves were obtained to prove the electrical properties of the HOPG/Monolayer/ C-FEBID device (Figure 4).

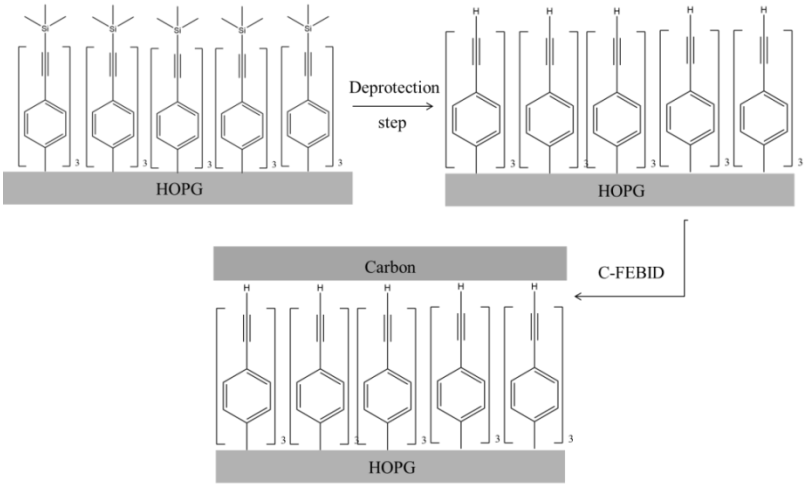

Figure 4. All carbon HOPG/Monolayer/Carbon device fabrication.

3. Experimental section

The equipment and methodology used in this work is presented below.

3.1. Equipment

- Potentiostat/Galvanostat AUTOLAB PGSTAT302N, which belongs to the PLATON research group. It is located in the Physical Chemistry department of the Science Faculty building. An electrochemical cell Metrohm 6.1415.210. was used.
- SPM Multimode 8 from Veeco-Bruker environmental microscope that belongs to the Laboratory for Advanced Microscopies (LMA: lma.unizar.es). This microscope is located in the I+D+i building of Campus Río Ebro.
- XPS Kratos AXIS ultra DLD spectrophotometer with a monochromatic beam source Al K (1486.6 eV), that belongs to the LMA. The peaks are referred to the C(1s) peak at 284.6 eV.
- DUAL BEAM Helios Nanolab 650 that belongs to the LMA, located in the Clean room of the Institute of Nanoscience of Aragon (INA). The equipment allows the Focused Electron Beam Induced Deposition of carbon and also to record the electric measurements with a microtips Kleindiek® system.
- RAMAN WITEC Alpha 300M+ with different magnifiers of 10x, 20x, 50x and 100x. This instrument belongs to the INA.
- Ultrasounds J.P Selecta 3000583.
- Sartorius CP 225D Scales.

3.2. Reagents and solvents

Table I shows the different reagents and solvents used in this work together with their CAS number, purity and supplier.

Table I. Reagents and solvents.

Compound	CAS number	Supplier	Purity
Tetraethylammonium tetrafluoroborate	429-06-1	Sigma-Aldrich	≥99.0%
Tert-butyle nitrite	540-80-7	Sigma-Aldrich	90%
NH_2-OPE-TMS	-	*	
Potassium chloride	7447-40-7	Fluka	99%
Sulfuric acid	7664-93-9	Fischer-chemical	95%
Acetonitrile (max. 0.001% H_2O).	75-05-8	Sigma-Aldrich	99.9%
Nitric acid	7697-37-2	NORMAPUR	65%
Milli-Q water	7732-18-5	Science Faculty	

* Synthesized in the laboratory of Prof. Paul J. Low from Western Australia University (Durham University before). The synthesis of this compound is described in reference.[13]

3.3. Substrates

Highly Ordered Pyrolitic Graphite (HOPG) has been used as the bottom electrode in this work. HOPG presents a smooth and flat surface with large terraces where the monolayer can be formed homogeneously and can be detailed studied by AFM.

3.4. Redox probes

- Potassium hexacyanoferrate (III). Scharlau. CAS: 13746-66-2. Purity: ≥99%
- 3,4-Dihydroxiphenilethylamine (Dopamine). Sigma-Aldrich. CAS: 62-31-7. Purity: 99,9%

3.5. Electrodes

- Counter electrode:Platinum sheet. Metrohm 6.0351.100

- Reference electrode in aqueous solutions:Ag/AgCl, 3M KCl. Metrohm 6.0733.100
- Reference electrode in organic solutions: $Ag/AgNO_3$. BASi MF-2062.

3.6. Diazonium salt synthesis

In 1978 Michael P. Doyle and William J. Bryker[14] proposed the diazonium salt synthesis by reduction of anilines in organic or aqueous media. Since the diazonium salts are expensive and not stable with time, an "*in situ*" reduction process of the TMS-OPE-NH_2 molecule was carried out in the same electrochemistry cell where the *electrografting* process took place. Following this procedure, we have used 20 mL of acetonitrile, ACN, which were added as solvent in the cell, where the final concentrations of the reagents were:

- 3 mM of tert-butyle nitrite as reductor.
- 0.1 M of tetraethylammonium tetrafluoroborate (TEATFB) as support electrolyte and reagent. The electrolyte was dried at 80 ºC in vacuum during 24 hours since this compound is very hygroscopic and the reaction must be carried out in the absence of water.
- 0.25 mM or 2.5 mM of TMS-OPE-NH_2 (the efficiency of the process has been studied in terms of the diazonium salt precursor as explained later).
- The reaction time was 30 minutes. The reaction was performed under stirring and N_2 flux to avoid the atmospheric oxygen. The reaction takes places in two steps: 1) formation of the reductor molecule of nitrosyl fluoride and 2) the reduction of the amine with the nitrosyl fluoride to a diazonium salt. The reaction mechanism for the first step is based in an attack of $[BF_4]^-$ to the nitrogen of the tert-butyl nitrite, obtaining nitrosyl fluoride and tert-butylate, that reacts later with water resulting in the formation of tert-butyl alcohol. The reaction mechanism for the second step is based in an attack of the amine to the nitrogen of the nitrosyl fluoride, with the elimination of the F^- and followed by the reduction to the diazonium salt with the formation of H_2O.

Once the reaction has taken place, the composition of the mixture is 0.25 or 2.5 mM in the diazonium salt, 2.75 mM or 27.5 mM tert-butyl nitrite and 0.1 M TEATFB. The

relation 3:1 reductor/amine is very important to avoid the coupling reaction between the diazonium cation and the amine, which results in a triazene.

3.7. Electrografting process

A careful cleaning process is required before the *electrografting* process. The HOPG substrates were washed in a mixture of Milli-Q water and nitric acid 1:1 for 3 minutes under sonication. Later, an exfoliation process with cello tape (2 or 3 times) is required to eliminate the first graphitic layer and finally the substrate was rinsed with ACN. As Daniel Belanger showed,[15] the "*in situ*" reduction process of diazonium salts does not interfere with the *electrografting* process.

When the current flows to the substrate an electron reacts with the diazonium salt, reducing the N_2^+ group, that is eliminated as $N_2(g)$ from the mixture, obtaining an aryl radical in para- position.[16] This radical reacts with the substrate, obtaining a covalent bond with the surface. This process forms a layer that blocks the electrode, avoiding the current flow from the substrate to the solution.

All the electrografting reactions and electrochemistry characterizations were carried out at a scan rate of 50 $mV \cdot s^{-1}$, with a step potential of 0.01 V, applying cathodic scans. The reference potential of Ag/Ag^+ in ACN is 0.457 V versus the hydrogen normal electrode.

The electrochemistry area of all the substrates was calculated to obtain information of current density, *j*, applying the Randle-Sevcik equation. More information about the procedure to determine the electrode area can be found in Annex 1.

3.8. Atomic Force Microscopy characterization

AFM images were obtained by a Multimode microscope 8 (Veeco), equipped with a control unit Nanoscope V (Bruker), in environmental conditions with a scan rate of 1.0-1.2 Hz. The samples were characterized in Tapping™ mode, using FESP tips (60-100 kHz, 1-5 $N \cdot m^{-1}$, Bruker). To measure the thickness of the *electrografting* films 5 different *scratchs* were done in different areas of the modified surface. RTESP tips (271-311 kHz, 40-80 $N \cdot m^{-1}$, Bruker) were used in contact mode with a force range of 1-5 μN.

3.9. Focused Electron Beam Induced Deposition procedure

In FEBID, a Scanning Electron Microscope (SEM) decomposes precursor molecules, giving a solid deposit and volatile fragments. Appling a control over the precursor and e-beam, it is possible to use this process to grow a carbon deposit onto a substrate. The use of this carbon deposits for the creation of low resistance electrical connection between carbon nanostructures has been proved.[17] In this work, C-FEBID top-contact electrodes were obtained with a DUAL BEAM HELIOS 650 in the Clean Room of INA, where the carbon top contact electrode comes from a naphthalene ($C_{10}H_8$) gas precursor. The equipment works at vacuum, with a base pressure of 6 x 10^{-6} mbar and a work pressure of 1 x 10^{-5} mbar. The e-beam was under a voltage acceleration of 5 kV and a 26 nA beam current was used to fabricate the carbon top-contact electrodes.

4. Results and discussion

4.1. Improvement and characterization of the monolayer: electrochemistry, AFM, RAMAN and XPS

A first set of experiments was carried out using a TMS-OPE-NH_2 concentration of 0.25 mM and a different number of voltammetric cycles. The *electrografting* voltammogram (Figure 5) shows a large current step from the first cycle to the second. This means that the *electrografting* process is functionalizing the surface during the first cycle and later, the trimethylsilane group avoids the subsequent *electrografting* deposition over the position 3 and 5 of the aromatic ring for the next cycles, preventing the multilayer formation.

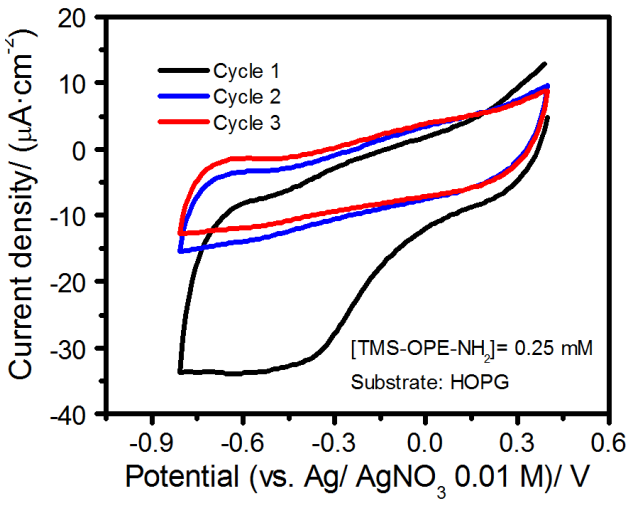

Figure 5. Cyclic voltammograms recorded upon the *electrografting* process of TMS-OPE-NH_2 onto a HOPG electrode. Conditions: [TMS-OPE-NH_2] = 0.25 mM, scan rate: 50 $mV \cdot s^{-1}$and [TEATFB] = 0.1 M as the supporting electrolyte.

Cyclic voltammetry can also be used as an indirect method to detect the presence of defects or holes in the film.[18] The redox probes that have been used to do this CV experiments are: potassium hexacyanoferrate (III), dopamine. An electrochemical description of these redox probes can be found in detail in annex 2.

The CV characterization process (Figure 6) using potassium hexacyano ferrate (III) as redox probe was done in aqueous media in the presence of 1 mM $K_3Fe(CN)_6$ and 0.1 M KCl as supporting electrolyte. The substrates modified by a different number of *electrografting* cycles were studied, but once the substrate was modified with three *electrografting* cycles (red line), the electrode does not exhibit any electrochemical activity since the film completely blocks the electron transfer.

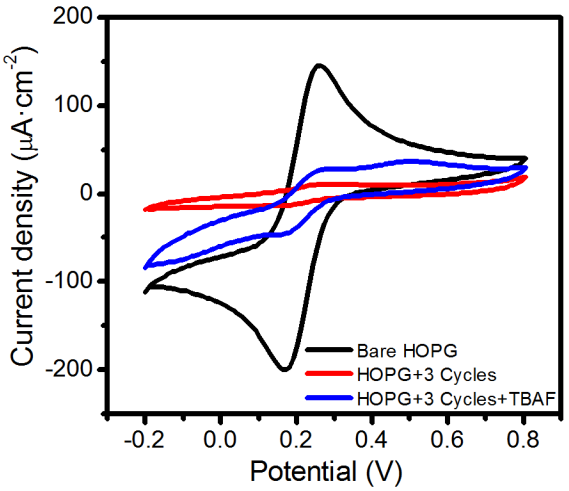

Figure 6. Cyclic voltammograms of $[Fe(CN)_6]^{3-}$ using a modified HOPG substrate with TMS-OPE-NH_2 deposited by *electrografting*. Conditions: $K_3[Fe(CN)_6]$ = 1 mM , scan rate: 50 mV·s^{-1}, KCl = 0.1 M

Another technique to analyze the films formed by the *electrografting* process is the XPS. This technique provides information about the presence or absence of nitrogen in the electrografted films. Figure 7 shows the XPS spectrum of TMS-OPE-NH_2 powder and the electrografted films obtained from this molecule. The nitrogen atom is not present in the electrografted film from TMS-OPE-NH_2 which reveals that the molecules have been converted into the diazonium salt and conveniently electrografted onto the HOPG substrate.

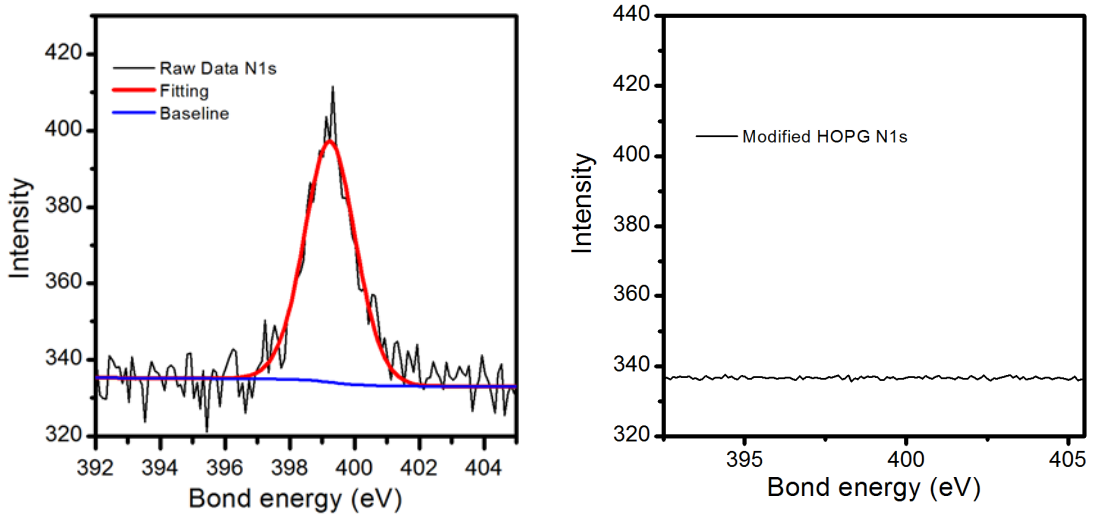

Figure 7. Left: XPS spectrum of TMS-OPE-NH_2 powder in the N1s region. Right: XPS spectrum of the electrografted film from TMS-OPE-NH2 onto HOPG in the N1s region.

Further information about the nature and the morphology of the modified HOPG substrates has been obtained by AFM. AFM images for films without the deprotection step (Figure 8) show a homogeneous layer with a very low Root Mean Square (RMS) of 0.378 nm ± 0.026 nm.

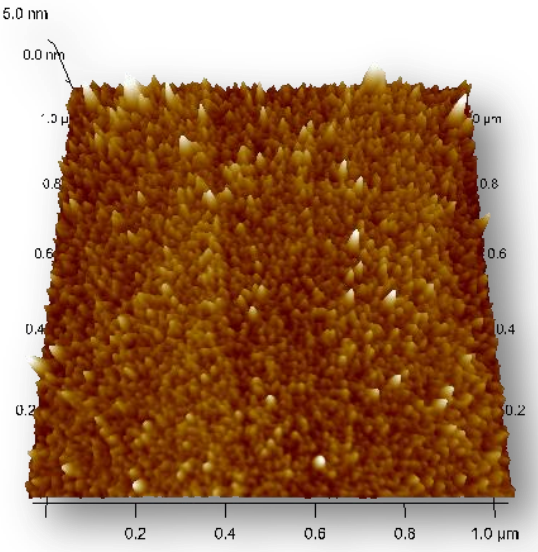

Figure 8. 3D AFM image of a film of 3 *electrografting* cycles on HOPG.

To measure the thickness of the layer, different scratches (Figure 9) were done and were compared with the theoretical height of the molecule, h = 2.2 nm, determined using a molecular model (Chem3D 13.0.0.3015). In this case the thickness, t = 4.01 nm ± 0.22 nm, corresponds to the height of two molecules, i.e. a bilayer.

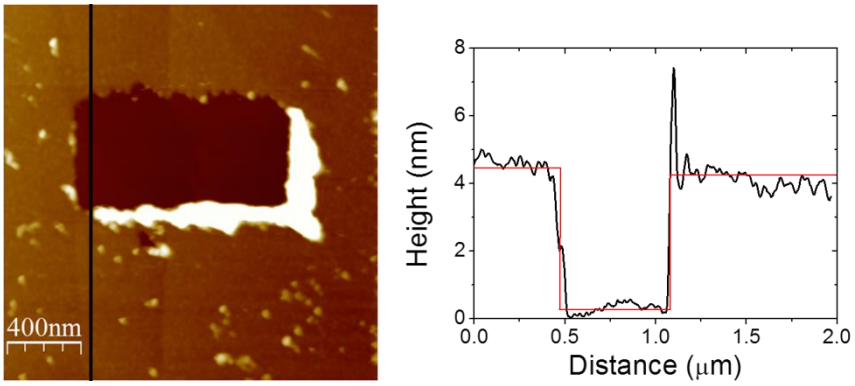

Figure 9. AFM scratch of a film of 3 *electrografting* cycles on HOPG (left) and section profile (right).

Once the substrate was modified, a deprotection step with tetra-n-butylammonium fluoride (TBAF) 50 mM in ACN was done to remove the TMS group. When the deprotection step is applied, two kinds of peaks appear (blue line in Figure 6) in the CV recorded using hexacyano ferrate (III) as the redox probe, exhibiting a higher current density than the voltammograms of films with the TMS group (Figure 6). These peaks (amplified in Figure 10) have been attributed to the presence of holes (blue dot lines in Figure 10), that appear when the deprotection step is applied, and electron transfer through the layer by tunneling current (red dot lines in Figure 10) to the redox probe. The reduction and oxidation peaks attributed to the presence of holes in the film appear closer (in volts) than the peaks attributed to the tunneling current. This is because a redox process that occurs in the interphase electrode surface/redox probe is more reversible than an electrode surface/layer/redox probe, which requires a higher voltage (a higher energy) to exceed the tunnel barrier of the layer.

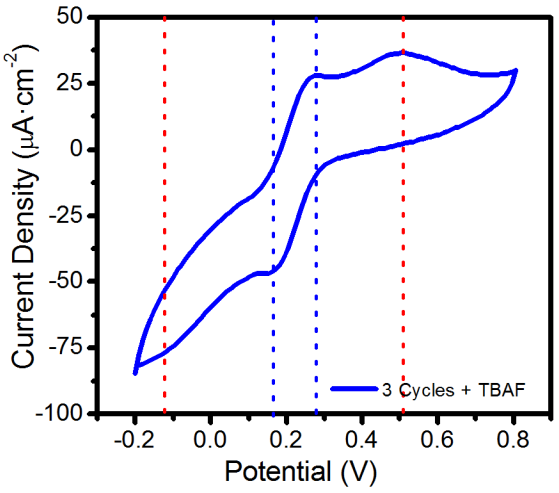

Figure 10. Cyclic voltammograms of $[Fe(CN)_6]^{3-}$ using a modified HOPG substrate with TMS-OPE-NH_2 deposited by *electrografting* and a deprotection step with TBAF is applied. Conditions: $K_3[Fe(CN)_6]$ = 1 mM, scan rate: 50 mV·s^{-1}, KCl = 0.1 M.

The assessment of the film quality by using dopamine as redox probe (Figure 11) was done in aqueous media employing a solution 1 mM in dopamine and 0.1 M in H_2SO_4. Similarly to the observations presented above with the $K_3[Fe(CN)_6]$ redox probe, once the

substrate is modified by applying three *electrografting* cycles the electrode is completely blocked and no faradaic current is observed (red line). Dopamine must be adsorbed onto the surface of the electrode to give a redox response. In this case (Figure 11), two kinds of peaks appear, one pair closer cathodic and anodic peaks, called G (green dot lines), than the other one, called M (magenta dot lines). G peaks could be due to the oxidation/reduction diffusion process of the dopamine redox probe through the holes of the layer, due to the reversibility and ease of the process. On the contrary, M peaks could be attributed to the diffusion of the molecule through the layer. Since dopamine is a very small neutral molecule, it can penetrate between the molecules of the layer and arrive at the surface of the substrate to give the redox response. Since the diffusion process is more difficult than penetration through holes in the film, it needs more energy, which explains why such peak appears at higher potentials than the holes.

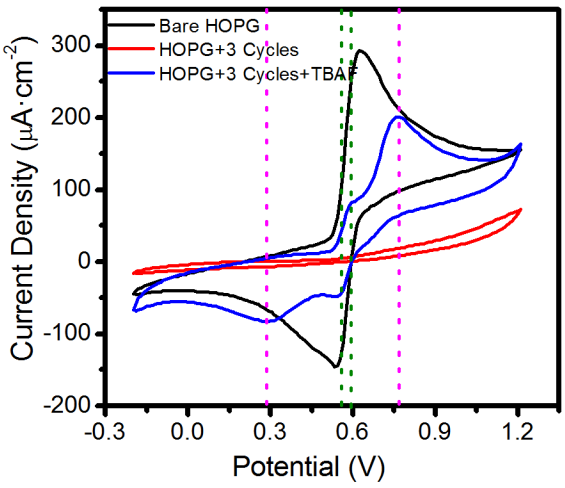

Figure 11. Cyclic voltammograms of dopamine on HOPG substrate modified with TMS-OPE-NH_2 by *electrografting*. Conditions: Dopamine = 1 mM, scan rate: 50 $mV \cdot s^{-1}$, H_2SO_4 = 0.1 M

AFM images (Figure 13) were recorded to study the morphology and the height of the layer after the deprotection step is applied. AFM images allow the determination of the thickness of the layer by scratching the film with the AFM tip. The thickness of the film after the deprotection step was t = 1.98 nm ± 0.19 nm, which corresponds to the thickness of a monolayer. Additionally, the obtained AFM images show the presence of the holes in the film after the deprotection step, which could be due to physisorbed molecules in the

pristine film, which are removed after the deprotection step. Since these physisorbed molecules are weakly bonded to the surface, and when TBAF eliminates the protector group, molecules can scape easily from the film when the washing process is applied, allowing the formation of holes.[9] These results are in agreement with the electrochemistry characterization above described that exhibited the presence of holes.

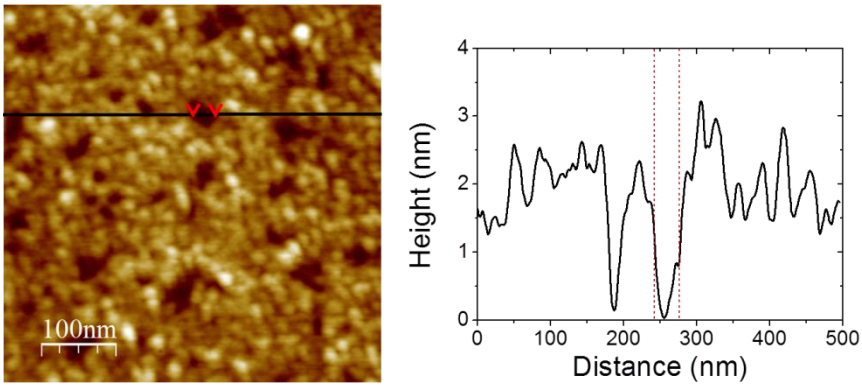

Figure 12. AFM image of a film fabricated by three *electrografting* cycles with the subsequentdeprotection step (left) and section profile (right). The two red marks indicate the presence of a hole.

A comparison of the AFM images before and after the deprotection step, indicate a transition from a bilayer to a monolayer. Also, the removal of physisorbed molecules results in the appearance of holes and a relatively low surface coverage of the HOPG surface as determined by means of a bearing analysis of the AFM image (Figure 14).

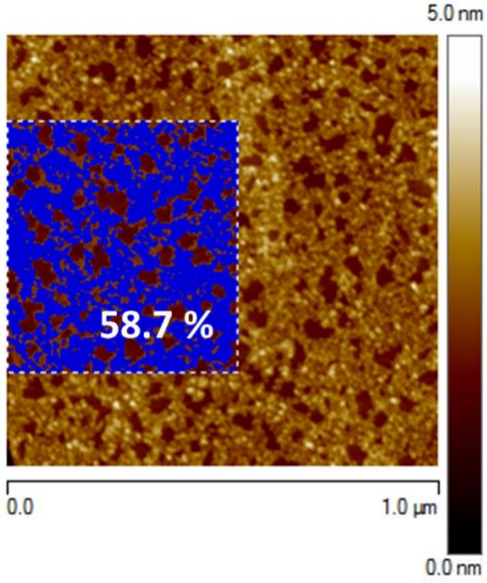

Figure 13. Surface coverage percentage determined by means of a bearing analysis of an AFM image corresponding to a HOPG substrate of a film prepared by three *electrografting* cycles with a subsequent deprotection step on HOPG.

Therefore, the deposition process of the molecules on the electrode needs to be improved in order to achieve a homogeneous monolayer with a higher surface coverage. To do so, two approximations were studied. The first one was to use a higher concentration of the diazonium salt, M = 2.5 mM and applying a cleanliness process between consecutive *electrografting* processes. It is known that an increase in the initial concentration of the diazonium salt precursor, and therefore in the diazonium salt, results in a higher covalent modification of the surface.[9] To check the quality of the layer prepared using this protocol, CV using redox probes was performed once the deprotection step was applied. The CV (Figure 15) using $[Fe(CN)_6]^{3-}$ as redox probe shows a remarkable difference between the two concentrations used at 0.25 mM and 2.5 mM. When a high concentration is used (blue line) it only appears one oxidation/reduction peak, instead of two peaks at lower concentration (red line). This means that only an electron transfer mechanism occurs when a high concentration is used, which implies a decrease in the number of holes and an increase in the layer homogeneity.

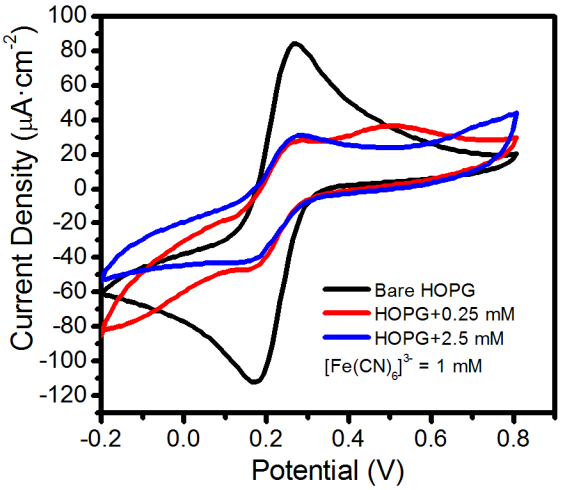

Figure 14. Cyclic voltammograms of $[Fe(CN)_6]^{3-}$ using as the working electrode a HOPG substrate modified with TMS-OPE-NH_2 by three *electrografting* cycles at the indicated concentrations of the diazonium salt followed by a deprotection step to remove the TMS group. Conditions: $K_3[Fe(CN)_6]$ = 1 mM , scan rate: 50 $mV \cdot s^{-1}$; KCl = 0.1 M

In the case of dopamine (Figure 16), the use of a concentration of 2.5 mM (blue line) of the TMS-OPE-NH_2 shows how the oxidation and reduction peaks attributed to the presence of holes (green dot lines) and those attributed to the diffusion through the layer (magenta dot lines) are more irreversible (wider peaks and with a larger potential difference between the anodic and cathodic peaks) than using 0.25 mM. This means a more compact layer that makes harder the diffusion through the layer and a reduction of the number of holes.

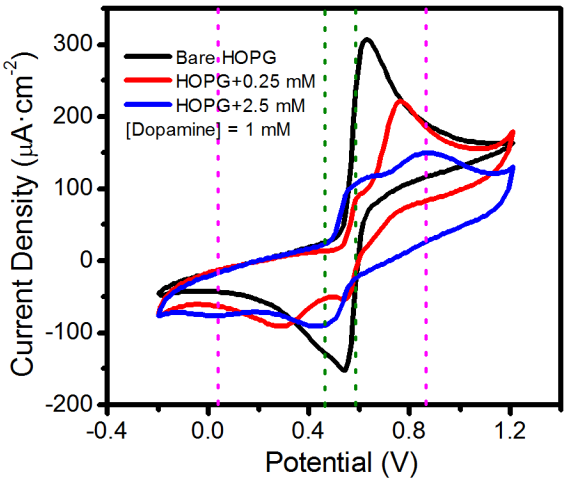

Figure 15. Cyclic voltammograms of dopamine using as the working electrode a HOPG substrate modified with TMS-OPE-NH_2 by three *electrografting* cycles at the indicated concentrations of the diazonium salt followed by a deprotection step to remove the TMS group. Conditions: Dopamine = 1 mM , scan rate: 50 $mV \cdot s^{-1}$ H_2SO_4 = 0.1 M.

To obtain qualitative information about the modification degree of a HOPG substrate due to the *electrografting* process, it is necessary a technique that provides information about the hybridization of the carbon atoms of the surface. RAMAN spectroscopy can provide information about the modification degree of a HOPG substrate. Thus, Figure X shows the RAMAN spectrum of a bare HOPG substrate, which exhibits two characteristic peaks, the first one the G-Band around 1576 cm^{-1} and the second one the 2D-Band, at 2680 cm^{-1}. The G-Band is attributed to the sp^2 carbon network that corresponds to the E_{2g} vibrational mode.[9] The 2D-Band is a second-order two-phonon mode. In contrast, modified HOPG substrates by *electrografting* of TMS-OPE-NH_2, show a D-Band, that corresponds to pristine or sp^3 carbon state. The *electrografting* process induces a transition from some C

atoms in the HOPG substrate from sp^2 to sp^3 when a covalent bond with the anchoring molecule is formed. This is the reason why a new band appears after the modification of the HOPG by the *electrografting* process, and it can be used to see the covalent modification of the surface (Figure 16). When the two substrates modified by *electrografting* at different concentrations of the diazonium salt, 0.25 and 2.5 mM, are compared, the intensity of the D-band is higher for the film prepared using 2.5 mM than for the one using 0.25 mM. This result indicates an increase in the number of C-C covalent bonds formed on the surface when the concentration is increased.

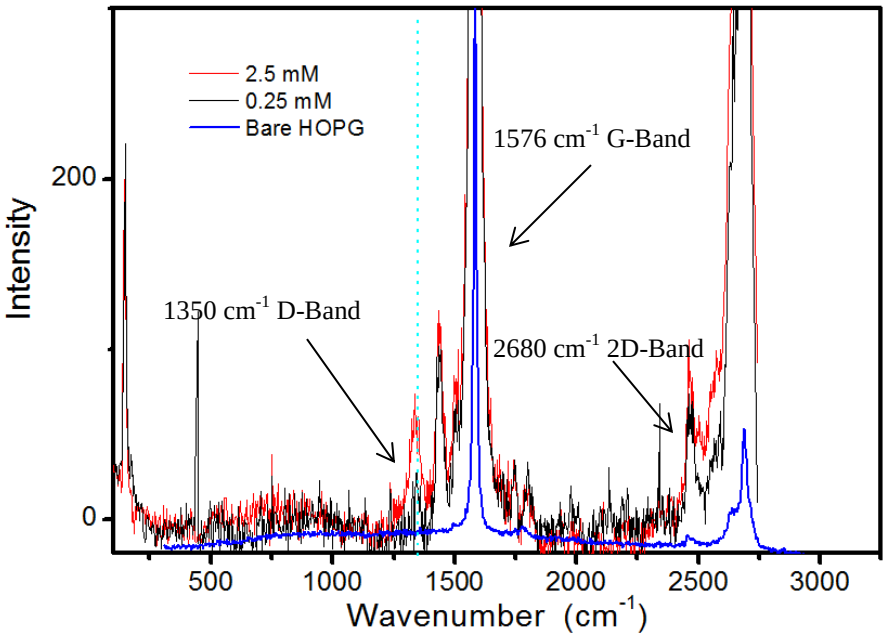

Figure 16. RAMAN analysis of HOPG modified by three *electrografting* cycles at different concentrations: 2.5 mM (red) and 0.25 mM (black) without applying deprotection step.

The second approximation used to improve the surface coverage of the monolayer was to apply a cleaning step between the *electrografting* cycles. The goal is to remove the weakly physisorpted molecules from the HOPG surface that are not covalent bonded. To remove these physisorbed molecules, several steps in the cleaning process were applied since these molecules strongly interact with neighbor molecules and therefore are difficult to eliminate. First the modified HOPG substrate was sonicated for five minutes in ACN. Then, it was rinsed with ethanol, acetone and finally with ACN. A noticeable difference in the electrochemical response of the modified electrodes fabricated with this cleaning

protocol between the electrografting cycles has been observed as illustrated in Figure 17. Thus, the second cycle (red voltammogram in figure 17) results in a higher current density (in absolute value) than in Figure 5 revealing that after a first voltammetric cycle followed by a cleaning process the coverage of the electrode is lower than without the cleaning process.

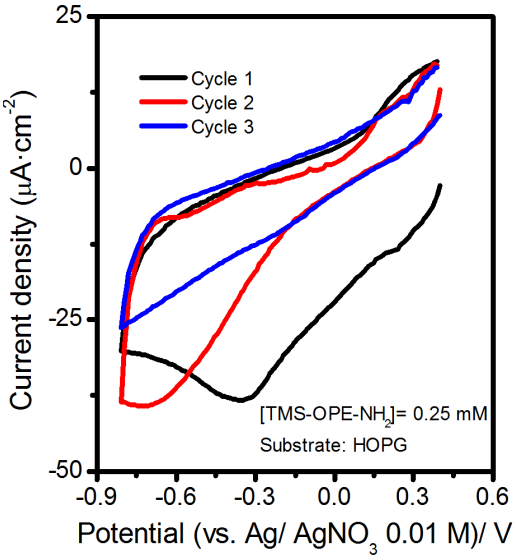

Figure 17. Cyclic voltammograms obtained upon the *electrografting* process applying the cleaning process described in the text between cycles. Conditions: [TMS-OPE-NH_2] = 0.25 mM, scan rate: 50 $mV \cdot s^{-1}$ and [TEATFB] = 0.1 M as the supporting electrolyte.

AFM images of the modified substrates prepared by successive cycles of *electrografting* and cleaning were taken. The topography image (Figure 18) shows a more compact layer with fewer pores than those obtained without the cleaning process between CV, which confirms the effectivity of the cleaning steps and the formation of a homogeneous layer.

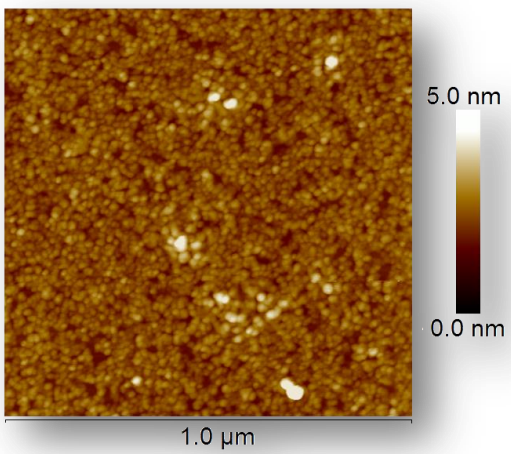

Figure 18. AFM image of a modified HOPG substrate by applying three *electrografting* cycles at 0.25 mM with cleaning steps between the *electrografting* cycles followed by the removal of the TMS group.

However, the cleaning processt is not enough to obtain a monolayer with the ideal characteristics to deposit a top-contact electrode due to the presence of large pores (Figure 19) on the surface and surface coverage of 71.2 %, which increases the probability of short-circuits when the top-contact is deposited.

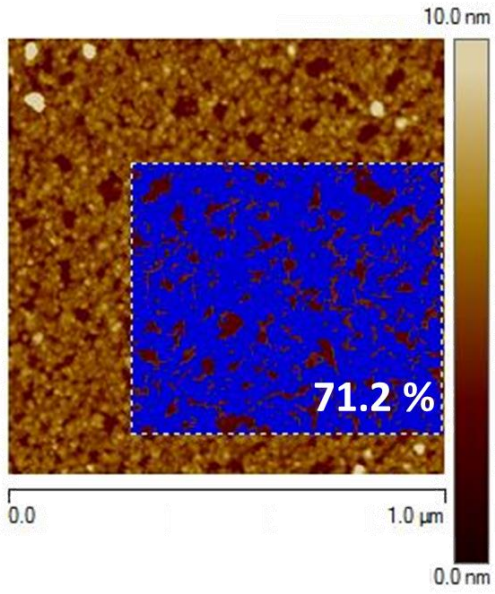

Figure 19. Surface coverage percentage determined by applying a bearing analysis to an AFM image of a film prepared by three *electrografting* cycles using a diazonium salt concentration of 0.25 mM with cleaning steps between successive *electrografting* cycles and subsequent removal of the TMS group.

Due to the efficiency of the two approximations, they were combined, using a high concentration of the TMS-OPE-NH_2 and the cleaning process (denominated S in Figure 20). The obtained films were characterized by CV and AFM as before. The cyclic voltammograms (Figure 20) using $[Fe(CN)_6]^{3-}$ as redox probe show how the electrode surface is more blocked than before (magenta line).

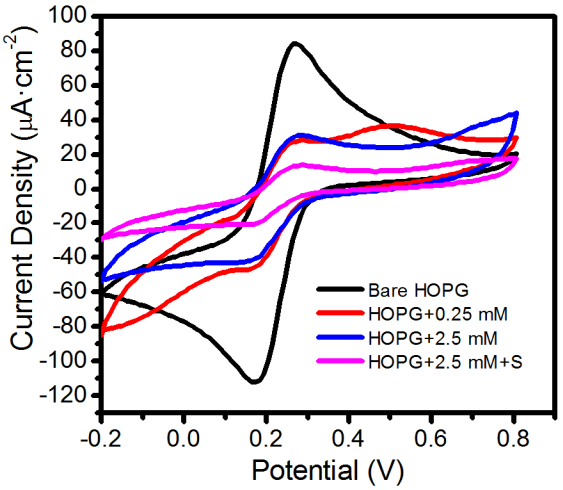

Figure 20. Cyclic voltammograms of $[Fe(CN)6]^{3-}$ probe using as the working electrode a HOPG substrate modified with TMS-OPE-NH_2 by three *electrografting* cycles using the indicated conditions followed by a deprotection step to remove the TMS group and comparison with a bare HOPG electrode. Conditions: $K_3[Fe(CN)_6]$ = 1 mM , scan rate: 50 $mV \cdot s^{-1}$, KCl = 0.1 M.

Using dopamine (Figure 21) as redox probe a reduction of the current density of the two kinds of peaks described above is observed. In the case of peaks attributed to the presence of holes, the intensity is very low. In addition, the peaks attributed to the diffusion of the dopamine through the film also exhibit a lower intensity and they are shifted to higher potentials, which indicates that the process is more difficult than before and then the layer must be more tightly packed.

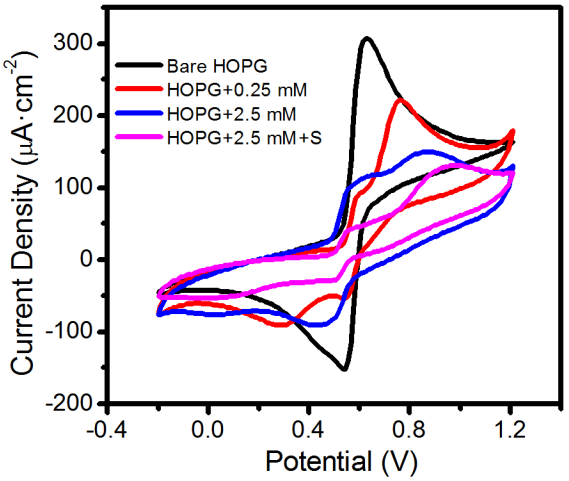

Figure 21. Cyclic voltammograms of dopamine using a modified HOPG substrate by three *electrografting* cycles followed by a deprotection step to remove the TMS group and comparison with the working electrode. Conditions: Dopamine = 1 mM , scan rate: 50 $mV \cdot s^{-1}$, H_2SO_4 = 0.1 M

To verify the presence of the protecting group on the modified HOPG electrode after the *electrografting* process as well as the removal of the TMS after the deprotection step is applied, XPS experiments (Figure 12) were recorded before and after the deprotection step with TBAF (cyan line in Figure 12).

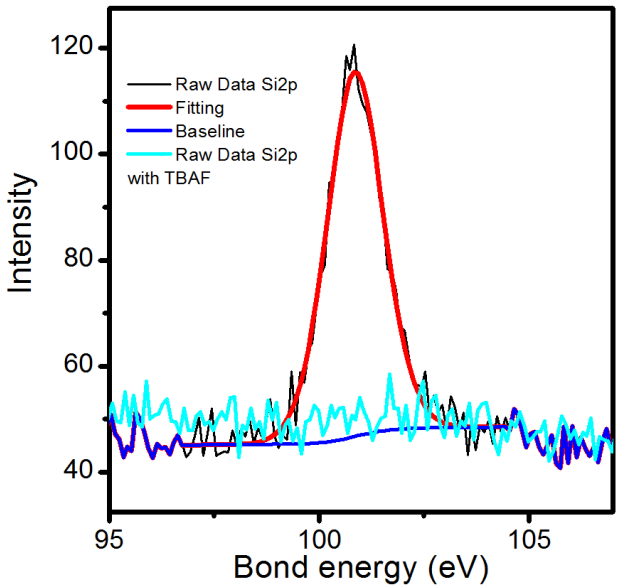

Figure 22. XPS data in the Si2p region of an electrografted film from TMS-OPE-NH_2 onto HOPG by 3 cycles of *electrografting* at 2.5 mM with cleaning process between every cycle.

The AFM image (Figure 23) of the film prepared by three electrografting cycles at 2.5 mM with cleaning steps between the electrografting cycles and deprotection step shows a homogeneous layer that covers the terraces of the HOPG substrate.

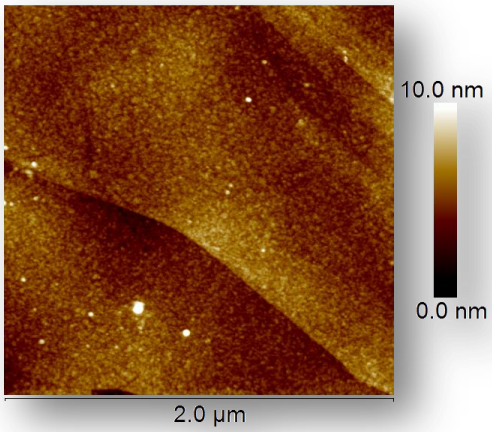

Figure 23. AFM image of a film of prepared by three *electrografting* cycles at 2.5 mM with cleaning steps between *electrografting* cycles and deprotection step on HOPG.

Once the combination of these two approximations is applied, there are few holes with a very low diameter. We consider that under these conditions the surface coverage percentage (Figure 24) is highly enough to perform the deposition of a top-contact electrode because the probability of having short-circuits is low.

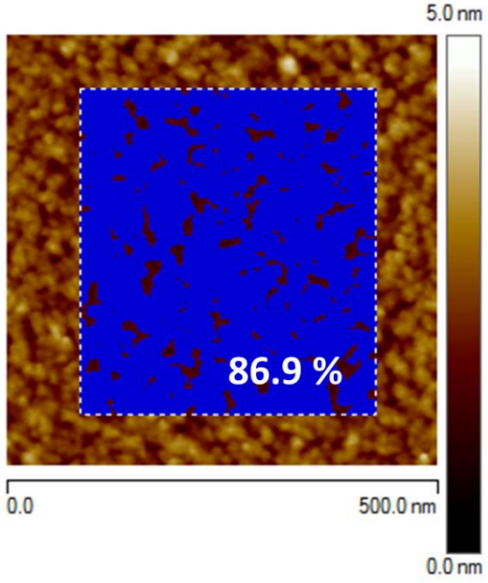

Figure 24. Surface coverage percentage determined by applying a bearing analysis to an AFM image of a film prepared by three *electrografting* cycles using a diazonium salt concentration of 2.5 mM with cleaning steps between successive *electrografting* cycles and deprotection step on HOPG.

4.2 FEBID and I-V Measurements

Carbon top-contact electrodes were fabricated by FEBID. Naphthalene ($C_{10}H_8$) was used as a precursor, which produces a controlled carbon-based deposit after its dissociation by the electron beam. Squared carbon deposits with an area of 5 x 5 μm^2 and a thickness of 31 nm were fabricated. To determine the electrical properties of the resulting all-carbon device HOPG/Monolayer/C-FEBID an additional platinum carbide layer (white areas of figure 25) was deposited to ensure the current flow through the entire top-contact carbon layer. Two *in situ* electrical microprobes were contacted: one of the electrical microprobes was placed on the platinum carbide and the second one onto the HOPG electrode.

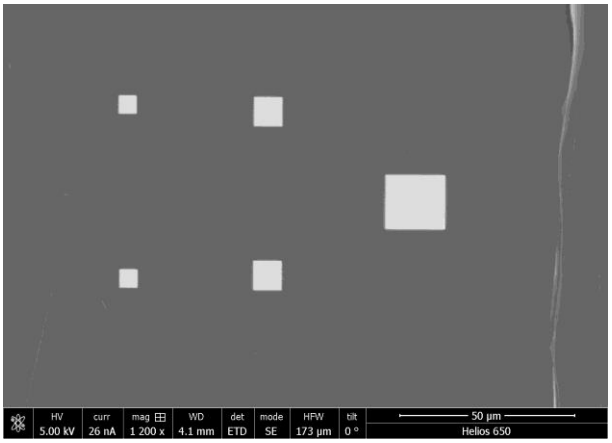

Figure 25. Platinum carbide deposits (white areas) onto the C-FEBID top-contact electrode.

Figure 26 shows *I-V* curves obtained for three different devices fabricated on the same *electrografted* film. The measurements of these three different devices are very similar to each other, demonstrating a high reproducibility of different steps involved in the fabrication process. The experimental *I-V* curves for the HOPG/Monolayer/C-FEBID shows a linear response between 0.25 V and -0.25 V voltage range and a nonlinear behavior for higher bias voltages. The nonlinear transport across OPE moiety was been previously observed,[19] with Scanning Tunneling Microscopy (STM) experiments, showing

that the transport through OPE fragments can be modelled in terms of transport across a tunneling barrier, by the Simmons expression[20] (Equation 1):

$$I = \frac{Ae}{4\pi^2\hbar s^2}\left\{\left(\Phi - \frac{eV}{2}\right)\exp\left[-\frac{2(2m)^{1/2}}{\hbar}\alpha\left(\Phi - \frac{eV}{2}\right)^{1/2}s\right] - \left(\Phi + \frac{eV}{2}\right)\exp\left[-\frac{2(2m)^{1/2}}{\hbar}\alpha\left(\Phi + \frac{eV}{2}\right)^{1/2}s\right]\right\}$$

Equation 1. Simmons expression.

where *A* is the area of the junction (5 × 5 μm^2 in our devices, equal to the area of the top electrode), *s* is the width of the tunneling barrier, Φ is the effective barrier height of the tunneling junction, *V* is the potential applied to the junction, α is a parameter related to the effective mass of the electrons in the tunneling process and *e* and *m* are the charge and the mass of the electron. Red lines of Figure 26 are the best fits obtained by using Equation 1 with the width of the tunneling barrier *s* being the value determined in the AFM experiments, 1.98 nm, and allowing Φ and α to behave as free parameters. For the three *I-V* curves shown in Figure 26, the best agreement between the experimental data and the Simmons model is found for Φ = 2.18 (a), 1.81 (b), 2.18 (c) and α = 0.86 (a), 0.95 (b), 0.86 (c). The values obtained for the effective tunneling barrier height modelling the transport across the devices based on electrografting process are in the same order of magnitude of the work function values in HOPG and C, around 5 eV. This implies that all the interfaces present in the devices are clean and flat and the *electrografted* monolayer forming the tunneling barrier is compact and almost defect-free: only when having a defect-free tunneling barrier as well as clean and flat interfaces in the junction, the effective tunneling-barrier height determined experimentally approaches that of the work function.

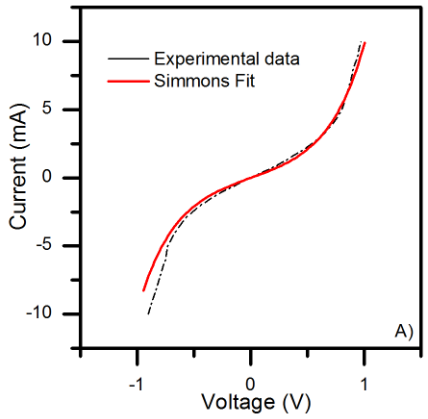

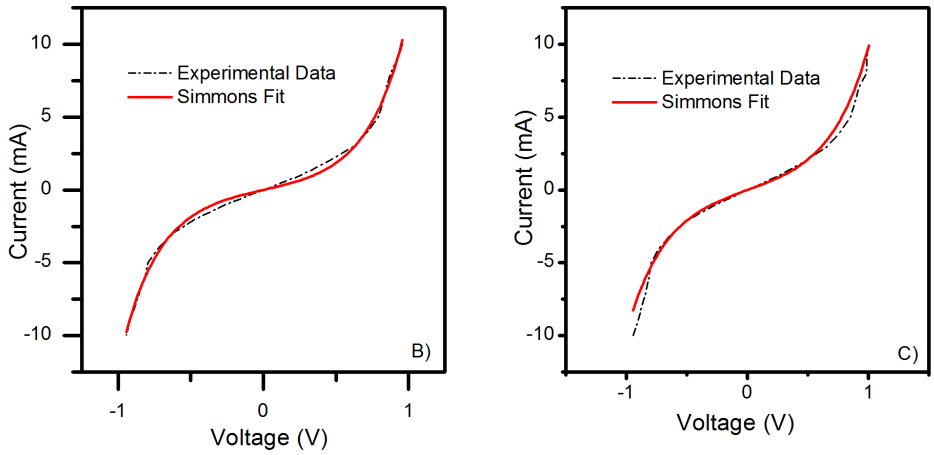

Figure 26. *I-V* curves of three all-carbon molecular electronic devices (a, b and c) fabricated on same *electrografting* monolayer onto HOPG, stressing the reproducibility in the growth of both the *electrografting* films and the top contact by FEBID.

5. Conclusions

In this work an optimization process has been described for the fabrication of an all-organic device HOPG/Monolayer/C-FEBID, using an electrografting process for the monolayer formation. It is important to highlight the fact that the electrografting process takes places in two consecutive steps but in the same flask, reducing time and costs. The layer was characterized by electrochemistry using different redox probes as well as by AFM, XPS and RAMAN. These characterization techniques indicate that the method used results in an excellent control of the film thickness and the formation of a homogeneous monolayer practically free of defects and holes. As it was reported in the literature the multilayer formation was a recurrent problem in the electrografting process. In this contribution the use of a bulky group in the 4 position of the terminal ring of the molecule has advantages versus other methods such as reduced cost, simplicity and the achievement of tightly packed monolayers. These metal-free devices lie in the emerging field of "green" electronics where the ultimate goal is to create paths for the production of environmentally friendly electronics. In addition, the results obtained for the effective barrier height are in good agreement with the literature. Thus applying this methodology all-organic electronic devices with possible uses in Molecular Electronics have been fabricated.

6. Bibliography

(1) Cavin, R. K. L., P.; Zhirnov, V. V. *Proceedings of the IEEE* **2012**, *100*, 1720.

(2) Editorial *Nature Nanotechnology* **2013**, *8*, 377.

(3) Ratner, M. *Nature Nanotechnology* **2013**, *8*, 378.

(4) Editorial *Nature Nanotechnology* **2013**, *8*, 385.

(5) McCreery, R. L.; Bergren, A. J. *Advanced Materials* **2009**, *21*, 4303.

(6) Cea, P.; Ballesteros, L. M.; Martín, S. *Nanofabrication* **2014**, *1*.

(7) Pinson, J.; Podvorica, F. *Chemical Society Reviews* **2005**, *34*, 429.

(8) Menanteau, T.; Levillain, E.; Downard, A. J.; Breton, T. *Physical Chemistry Chemical Physics* **2015**, *17*, 13137.

(9) Greenwood, J.; Phan, T. H.; Fujita, Y.; Li, Z.; Ivasenko, O.; Vanderlinden, W.; Van Gorp, H.; Frederickx, W.; Lu, G.; Tahara, K.; Tobe, Y.; Uji-i, H.; Mertens, S. F. L.; De Feyter, S. *ACS Nano* **2015**, *9*, 5520.

(10) Garcia, A. *Trabajo Fin de Grado* **2015**.

(11) Ballesteros, L. M.; Martín, S.; Pera, G.; Schauer, P. A.; Kay, N. J.; López, M. a. C.; Low, P. J.; Nichols, R. J.; Cea, P. *Langmuir* **2011**, *27*, 3600.

(12) Leroux, Y. R.; Hui, F.; Noel, J.-M.; Roux, C.; Hapiot, P. **2010**; Vol. 132, p 14039.

(13) Ballesteros , L. M.; Martín , S.; Cortés , J.; Marqués-González, S.; Higgins, S. J.; Nichols, R. J.; Low, P. J.; Cea , P. *Chemistry - A European Journal* **2013**, *19*, 5352.

(14) Doyle, M. P.; Bryker, W. J. *The Journal of Organic Chemistry* **1979**, *44*, 1572.

(15) Baranton, S.; Bélanger, D. *Electrochimica Acta* **2008**, *53*, 6961.

(16) Bélanger, D.; Pinson, J. *Chemical Society Reviews* **2011**, *40*, 3995.

(17) Konrad, R.; Matthew, R. H.; Song-Kil, K.; Andrei, G. F.; Dhaval, K.; Srikanth, S.; Vladimir, V. T. *Nanotechnology* **2010**, *21*, 035202.

(18) Villares, A.; Pera, G.; Giner, I.; Cea, P.; López, M. C.; Martín, S. *Journal of Chemical Education* **2009**, *86*, 723.

(19) Ballesteros, L. M.; Martín, S.; Marqués-González, S.; López, M. C.; Higgins, S. J.; Nichols, R. J.; Low, P. J.; Cea, P. *The Journal of Physical Chemistry C* **2015**, *119*, 784.

(20) Simmons, J. G. *Journal of Applied Physics* **1963**, *34*, 1793.